*Clays and Clay Minerals*, Vol. 45, No. 5, 649–658, 1997.

# INFRARED REFLECTANCE STUDY OF THERMALLY TREATED Li- AND Cs-MONTMORILLONITES

M. A. KARAKASSIDES,[1] D. PETRIDIS[1] AND D. GOURNIS[2]

[1] Institute of Materials Science, NCSR ⟨⟨Demokritos⟩⟩, 153 10 Ag. Paraskevi Attikis, Greece

[2] Institute of Physical Chemistry, NCSR ⟨⟨Demokritos⟩⟩, 153 10 Ag. Paraskevi Attikis, Greece

**Abstract**—The structure of Li- and Cs-montmorillonites was studied using infrared (IR) reflectance spectroscopy. The spectra of heat-treated clays between 80 and 220 °C were analyzed by Kramers–Krönig inversion in order to obtain the optical and dielectric properties of the clays. The analysis revealed the transverse-optic (TO) and longitudinal-optic (LO) components of the asymmetric stretching vibration of Si-O-Si bridges. Major differences, in particular the systematic development of new bands, were found in the Li-montmorillonite LO and TO spectra with increasing temperature. These changes were attributed to the migration of the Li-cations into the layer structure.

**Key Words:**—Cs-Montmorillonite, Li-Montmorillonite, Longitudinal-Optic (LO) Mode, Migration, Reflectivity, Transverse-Optic (TO) Mode.

## INTRODUCTION

IR spectroscopy in conjunction with other techniques has been extensively applied over the years to investigate the structure of layer silicates (Farmer and Russel 1964, 1967). Most IR studies of clay minerals refer to transmission measurements (Lerot and Low 1976; Sposito et al. 1983) and concern the effects on the transmittance spectra of clays modified by various processes such as intercalation, pillaring or adsorption of organic molecules. However, transmittance experiments present certain problems, such as the high absorptivities associated with minerals that make the recording of good quality transmission spectra difficult unless the mineral is less than 5 μm thick (Wihlborg 1989). Alternatively, the use of KBr pellets might create problems from a possible modification of the IR spectra due to ion exchange (Minami 1983) or randomly oriented specimens into the KBr matrix.

The specular reflectance method (mirror-like reflection from a solid surface) not only overcomes such problems but also offers a better analysis of the absorption spectra. The specular reflectance is often measured at or near normal incidence, where the reflected energy is small for those spectral regions where the material is nonabsorbing (5–10% for the most organic materials). However, strongly absorbing materials, such as many minerals and glasses, reflect radiation strongly over a specific energy range producing unique spectral features called rehststrahlen bands. An important advantage of the reflectance method is the unique analysis of the spectra. The analysis, realizable through the Kramers–Krönig transformation (Spitzer et al. 1962), leads to the calculation of the optical constants $n$ (real refractive index) and $k$ (dimensionless imaginary part of complex refractive index or extinction coefficient) as well as of the dielectric constants $\epsilon'$ and $\epsilon''$ of the medium. Most reflectance studies in clays have been focused on the high-IR frequencies (3000–8000 $cm^{-1}$) of the reflectivity spectra where the hydroxyl structural vibrations and the vibrations of interlayer water occur. In these studies, the reflectivity spectra were not analyzed, while structural information was obtained only from reflection or absorption features (Clark et al. 1990; Bishop et al. 1994; Delineau et al. 1994).

In the present work, specular reflectance spectroscopy was used to detect possible changes in the Si-O vibrations in the spectra of smectite clays as a result of the Hofmann–Klemen effect. The effect refers to the occupancy of the empty octahedral sites in a 2:1 phyllosilicate mineral by small cations such as $Li^+$, $Mg^{2+}$ after the cation-saturated clay is heated at 220 °C for at least 24 h (Hofmann and Klemen 1950). IR studies related to this effect (Calvet and Prost 1971; Russel and Fraser 1971; Sposito et al. 1983) have described the changes in the intensity and frequency of the stretching and bending vibrations of structural OH groups in Li-montmorillonites after the cation migration but not corresponding changes in the Si-O vibrations. Recent studies of the IR spectra of heat-treated Li-montmorillonites (Alvero et al. 1994; Modejová et al. 1996) have shown that the migration of $Li^+$ cations into the montmorillonite lattice affect the Si-O vibrations in the 950–1200 $cm^{-1}$ region. In this paper, the analysis of the IR reflectance spectra of Li- and Cs-montmorillonites by Kramers–Krönig transformation yields information about the optical and dielectric properties and vibrational modes of the clays. The results are discussed in relation to previously published data.

## MATERIALS AND METHODS

### Materials

The montomorillonite used in this study was supplied by the Clay Minerals Society from the source





https://doi.org/10.1346/CCMN.1997.0450504 Published online by Cambridge University Press

SWy-1, Crook Country, Wyoming. The samples were fractionated to <2 μm by gravity sedimentation and were purified by standard methods (King et al. 1987). The Li- and Cs-exchanged samples were prepared by immersing the clay into 1 *M* solutions of the corresponding metal chlorides. Cation exchange was completed by washing and centrifuging 4 times with appropriate solutions. The samples were then washed with deionized water, transferred into dialysis tubes in order to obtain Cl-free clays and dried at room temperature. Clay samples were heated at various temperatures for 24 h. Tetraethyl orthosilicate (TEOS) was partially hydrolyzed in an ethanol solution with the stoichiometric amount of water (TEOS:ethanol:water = 1:1:4) and a few drops of $HNO_3$ as catalyst. The mixture was stirred for 24 h at room temperature, then left covered at temperatures between 40 and 50 °C until gelation occurred (approximately 48 h). The gel was gradually heated to 400 °C in order to obtain organic-free material.

### Spectral Measurements

IR reflectance spectra were measured with a Nicolet 550 IR spectrometer in the region 400–4000 $cm^{-1}$ equipped with a deuterated triglycine sulphide (DTGS) detector. Each spectrum was the average of 100 scans collected at 2 $cm^{-1}$ resolution, by means of a variable-angle attachment provided by SPECAC, Inc. All spectra were measured at room temperature, using unpolarized radiation at incidence angle 10° off-normal, against a high reflectivity aluminium mirror. The samples were ground and pressed in pellet form in order to obtain regularly flat surfaces suitable for specular reflectance measurements.

### Kramers–Krönig Analysis

The reflectivity data were analyzed by means of the Kramers–Krönig transformation (Spitzer and Kleinman 1961) in order to derive the optical and dielectric constants of the clays. In addition, the same analysis allows calculation of absorbance spectra from measured reflectance spectra (Kamitsos et al. 1990). A brief outline of the analysis of the reflectance spectra is given below.

The propagation of an electromagnetic wave into the vacuum is described by the equation:

$$E = E_o \exp[i(\mathbf{q}.r - \omega t)] \quad [1]$$

where $E_o$ is the amplitude of the wave, i is an imaginary number, $\mathbf{q}$ is the wave vector that is perpendicular to $E_o$, $\omega$ is the angular frequency, $r$ is the distance and $t$ is the time. The magnitude of the wave vector (wave number) is given by the known relation $\mathbf{q} = \omega/c$, where $c$ is the speed of the wave in the vacuum. When an electromagnetic wave passes from vacuum into an isotropic medium, the wave number of the medium $\mathbf{q}_m$ is related to the wave number of the vacuum by the equation:

$$\mathbf{q}_m = n^*\mathbf{q} \quad [2]$$

where $n^*$ is the complex refractive index of the medium and is given:

$$n^* = n + ik \quad [3]$$

where $n$ is the refractive index and $k$ is the extinction coefficient of the medium (optical constants of the medium).

If $E_i$ and $E_r$ are the incident and reflected waves to a solid surface, then the complex amplitude of the reflected wave is defined as:

$$r(\omega) = E_i/E_r = \rho(\omega)\exp[i\theta(\omega)] \quad [4]$$

where $\rho(\omega)$ is the amplitude and $\theta(\omega)$ is the phase difference between the incident and reflected waves. In the case of normal incidence, the well-known Fresnel formula is valid:

$$r(\omega) = (n^* - 1)/(n^* + 1) = (n + ik - 1)/(n + ik + 1) \quad [5]$$

where $n$ and $k$ are the real and imaginary parts of the complex refractive index. Equation [5] relates the reflectance amplitude to the optical constants $n$ and $k$ of the material. From equations [4] and [5], Equations [6] and [7] are easily derived.

$$n = (1 - \rho^2)/(1 + \rho^2 - 2\rho\cos\theta) \quad [6]$$

$$k = 2\rho\sin\theta/(1 + \rho^2 - 2\rho\cos\theta) \quad [7]$$

The quantity measured in a specular reflectance experiment is the reflectivity of the sample $R(\omega)$, which is defined as the ratio of the reflected to the incident intensities:

$$R(\omega) = I_r/I_i = E^*_r E_r/E^*_i = r^*r = \rho^2 \quad [8]$$

$$\text{and } \rho(\omega) = [R(\omega)]^{1/2} \quad [9]$$

Knowing the reflectivity $R(\omega)$, $n$ and $k$ may be calculated from Equations [6] and [7] if the phase difference $\theta(\omega)$ of the reflected wave is known. The phase difference $\theta(\omega)$ can be determined if $R(\omega)$ is known for all frequencies. The calculation is possible through the Kramers–Krönig transformation (KK), which gives the real part of the response of a linear system if the imaginary part is known for each frequency and vice versa. Based on Equations [4] and [9], it is seen that:

$$\ln r(\omega) = \ln R^{1/2}(\omega) + i\theta(\omega) \quad [10]$$

where the real part $\ln R^{1/2}(\omega)$ is related to the imaginary part $\theta(\omega)$ by means of the KK equation:

$$\theta(\omega_i) = 2\omega_i/2\pi \int_0^\infty ([\ln[R(\omega)]^{1/2} - \ln[R(\omega_i)]^{1/2}]\, d\omega)/(\omega_i^2 - \omega^2) \quad [11]$$

https://doi.org/10.1346/CCMN.1997.0450504 Published online by Cambridge University Press

The above integral can be computed for each angular frequency of interest $\omega_i$. However, the reflectivity, $R$, must be known for all frequencies, that is, from zero to infinity. This is not possible, hence extrapolations must be made that increase the uncertainty close to the limits of the experimental interval. Thus the KK transformation was performed after appropriate extrapolations of the reflectance data at $\omega \rightarrow 0$ and $\omega \rightarrow \infty$. Once the spectrum of the phase difference $\theta(\omega)$ is calculated, the real ($n$) and imaginary ($k$) parts of the refractive index can be obtained from Equations [6] and [7]. On the other hand, the refractive index, $n^*$, is related to the complex dielectric permittivity $\epsilon^*(\omega)$ by the Maxwell equation:

$$n^*(\omega) = (\epsilon^*(\omega))^{1/2} \quad [12]$$

$$\epsilon^*(\omega) = \epsilon'(\omega) + i\epsilon''(\omega) \quad [13]$$

where $\epsilon'$ and $\epsilon''$ are the real and imaginary parts of the complex dielectric permittivity $\epsilon^*(\omega)$, respectively. By combining Equations [3], [12] and [13], the expressions for $\epsilon'(\omega)$ and $\epsilon''(\omega)$ are obtained as:

$$\epsilon'(\omega) = n^2(\omega) - k^2(\omega) \quad [14]$$

$$\epsilon''(\omega) = 2n(\omega)k(\omega) \quad [15]$$

which relate the optical to dielectric constants, respectively. Having determined the frequency-dependent refractive index $n$, and the extinction coefficient $k$, the $\epsilon'(\omega)$ and $\epsilon''(\omega)$ can be obtained from Equations [12] and [13]. The optical and dielectric constants are then used to calculate the absorption coefficient:

$$\alpha = 4\pi\omega k = (2\pi\omega\epsilon''(\omega))/n \quad [16]$$

and finally the energy loss function, Im, defined as the imaginary part of $1/\epsilon$ where $\epsilon$ is the complex dielectric permittivity, is given by:

$$\mathrm{Im}(-1/\epsilon^*(\omega)) = 2n(\omega)k(\omega)/(n^2(\omega) + k^2(\omega))^2 \quad [17]$$

## RESULTS AND DISCUSSION

A representative example of a such KK analysis of a reflectance spectrum is shown in Figure 1 for a Li-montmorillonite sample dried at 80 °C. The recorded reflectance spectrum at near-normal incidence (10° off-normal) shows the strongest reflectivity at high frequencies where a strong band at 1065 $cm^{-1}$ and a weaker feature at 1130 $cm^{-1}$ are observed, Figure 1a. Theory predicts that, in an ionic crystal, there is a maximum in the intensity of the reflection and that the position of this maximum is close to the wavelength of the absorption. However, the maxima occurring in the reflection spectrum of a substance possessing dispersion bands result from the combined effects of the changes in both the refractive index ($n$) and the extinction coefficient ($k$). Thus, the observed reflectivity maxima are not located exactly at the frequency of lattice vibrations. Alternatively, the vibrational spectrum of a crystal contains branches that correspond to sound waves in the crystal (acoustical branches) and branches with frequencies of the order of about $10^{13}$ $sec^{-1}$ which correspond to motions of the atoms in opposite directions. These latter modes, called optical modes, produce a strong polarization in ionic crystals and interact strongly with electromagnetic radiation (transverse modes) and with charged particles (longitudinal modes; Stern 1963). Transverse optical modes are those in which the electric field, $E$, is perpendicular to the direction of periodicity of the wave, and longitudinal those in which the $E$ is parallel. In clays, by analogy with crystalline or amorphous silicates (Galeener and Lucovsky 1976; Kamitsos et al. 1990), we can associate the maxima in $\epsilon''(\omega)$ and $\mathrm{Im}(-1/\epsilon^*)$ with TO and LO vibrations. Figures 1b–1e show the $\epsilon''(\omega)$ and $\mathrm{Im}(-1/\epsilon^*)$ spectra, the optical constants $n$ and $k$ spectra and the absorption coefficient spectrum, all obtained from the KK analysis of the Li-montmorillonite spectrum of Figure 1a.

It should be noted that, according to Equation [16], the TO vibrations correspond approximately to the maximum of the absorption coefficient. This is indicative that IR absorption spectroscopy gives only the TO modes, in contrast to reflectance spectroscopy, which yields both the TO and LO components of each vibrational mode. In fact, when IR radiation falls normal to the sample surface, only the TO modes can be detected, owing to the transverse character of electromagnetic radiation. However, Berreman (1963) has shown that, in thin films, both modes can be detected in oblique incidence. In that case, the parallel component of radiation of oblique incident will have electric field components perpendicular and parallel to the film surface that can create the LO and TO modes. Recently, Almeida et al. (1990) have shown that the above argument for transmission through thin crystal films can be extended to reflection from bulk vitreous $SiO_2$ and so probably from samples in the form of pressed pellet, as we use in this study.

Figure 1e shows the Li-montmorillonite absorption coefficient spectrum derived from the analysis. The absorbance spectrum measured by KBr matrix method is also included for comparison. The calculated absorption coefficient spectrum is a good match based on peak positions and relative peak heights. This comparison shows that the KK analysis is a useful tool for comparing specular reflectance data with measured absorbance or transmittance data. In this study, we prefer to present and discuss our data in the form of optical and dielectric constants versus frequency, since it is the first time that such data on clay minerals are reported. However, since most of the existing IR data on clay minerals are in the form of absorption or transmittance spectra, in a coming publication we will present reflectance results in the form of absorption coefficient.

https://doi.org/10.1346/CCMN.1997.0450504 Published online by Cambridge University Press

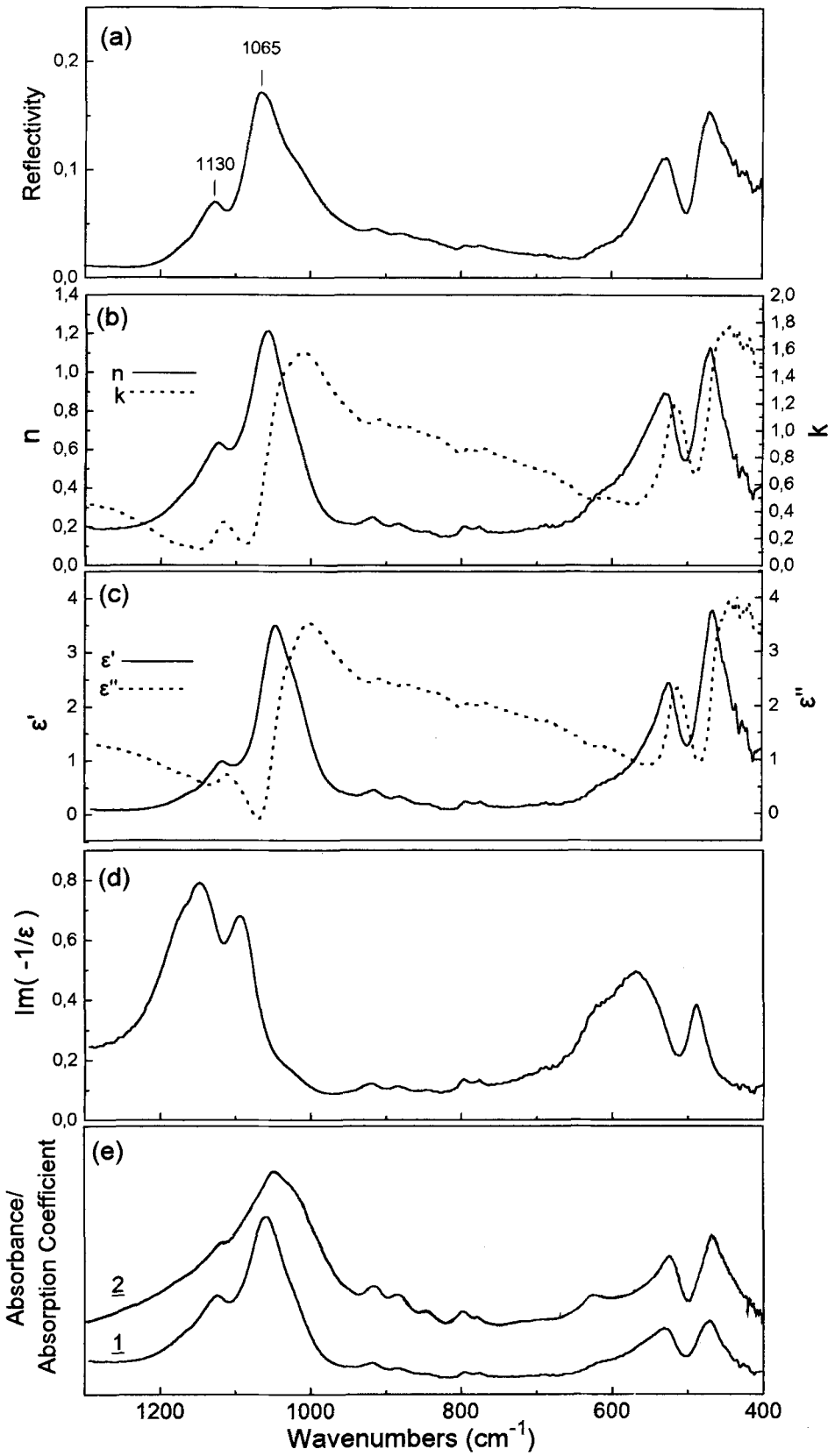


https://doi.org/10.1346/CCMN.1997.0450504 Published online by Cambridge University Press

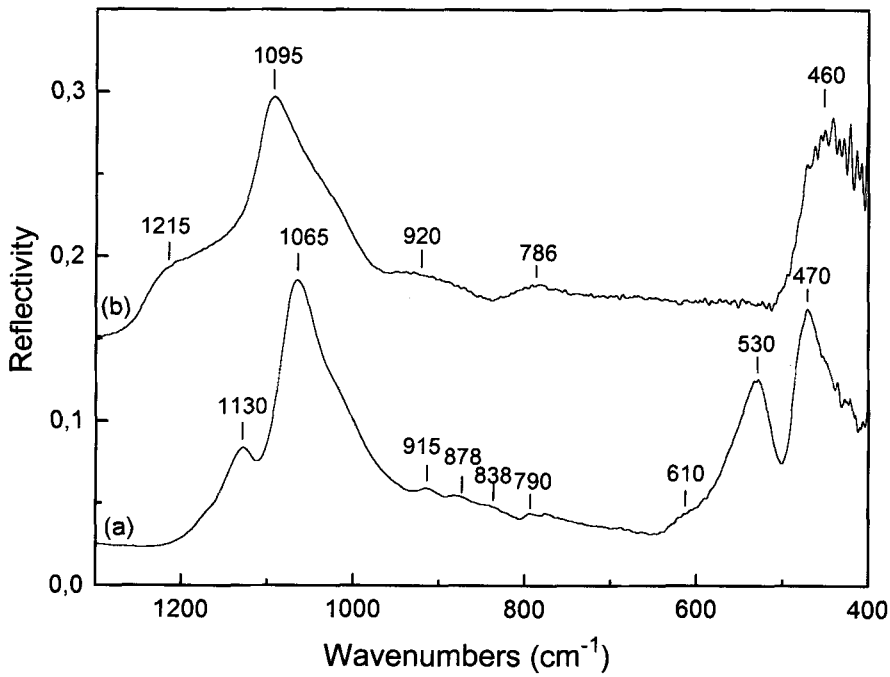


Figure 2. Reflectance spectra of Li-montmorillonite (a) and $SiO_2$ gel (b).

Figures 2a and 2b show the reflectance spectrum of Li-montmorillonite and the spectrum of $SiO_2$ gel for comparison. The IR spectra of the 2 materials show certain differences. Most of these differences in the spectra are expected because the clay lattice, as containing $MgO_4(OH)_2$, $FeO_4(OH)_2$ and mainly $AlO_4(OH)_2$ octahedra, is more complicated than the spectrum of $SiO_2$ gel. The reflectivity peaks in the $SiO_2$ gel spectrum are broader due to the amorphous character of the gel. The spectrum of the gel, Figure 2b, shows a strong peak at 1095 $cm^{-1}$ and a shoulder at 1215 $cm^{-1}$. The strong absorption at 1095 $cm^{-1}$ has been assigned to the TO component of the asymmetric vibration of the Si-O-Si bridges and the shoulder at 1215 $cm^{-1}$ to the LO component of the same vibration (Almeida et al. 1990). Similarly, the reflectivity spectrum of the Li-clay, Figure 2a, shows a pair of bands in the same region but shifted to lower frequencies (1130 and 1065 $cm^{-1}$) and with a smaller splitting between them. The similarity in the IR spectra, as shown in Figures 2a and 2b, supports the assignment of the 1130 and 1065 $cm^{-1}$ bands in the clay spectrum to the Si-O-Si asymmetric stretching vibrations perturbed by the presence of the Al, Fe and Mg ions in the octahedral layer. Such a perturbation can cause downshift in the peak frequencies of the asymmetric Si-O-Si stretching vibrations compared to the same vibrations of a pure Si-O tetrahedral network (Roy 1987). In addition, the clay spectrum exhibits 2 bands at 610 and 530 $cm^{-1}$ which are absent in the $SiO_2$ gel spectrum. These bands have been attributed to octahedrally coordinated Al(III) in the clay structure (Farmer 1974). The broad band appearing at 920 $cm^{-1}$ in the $SiO_2$ gel spectrum has been assigned to stretching vibrations of the Si-OH groups (Almeida et al. 1990). In the same region, the spectrum of the Li-clay exhibits 3 discrete bands which can be assigned to the bending vibrations of the OH groups binding the various octahedral units in the clay lattice: AlOHAl (915 $cm^{-1}$), AlOHFe (878 $cm^{-1}$) and AlOHMg (838 $cm^{-1}$). Finally, in the $SiO_2$ gel spectrum, the band at 786 $cm^{-1}$ has been assigned to the bending motion of oxygen atom along the bisector of the Si-O-Si bridging group, while the 460 $cm^{-1}$ reflection has been assigned to the rocking motion of the oxygen atom about an axis perpendicular to the Si-O-Si plane (Lucovsky et al. 1983; Kirk 1988; Almeida et al. 1990). These bands appear at almost the same frequency in the spectrum of Li-montmorillonite (790 and 470 $cm^{-1}$) and are ascribed to similar vibrations of the Si-O-Si bridges of the clay lattice. (As sug-

←

Figure 1. Kramers–Krönig analysis for the reflectance spectrum of the Li-montmorillonite: (a) reflectivity, (b) refractive index $n$ (·····) and extinction coefficient $k$ (———), (c) dielectric constants $\epsilon'$ (·····) and $\epsilon''$ (———), (d) energy loss function, $\mathrm{Im}(-1/\epsilon)$, (e) absorption coefficient (1) and absorbance spectrum (2) obtained in KBr matrix.

https://doi.org/10.1346/CCMN.1997.0450504 Published online by Cambridge University Press

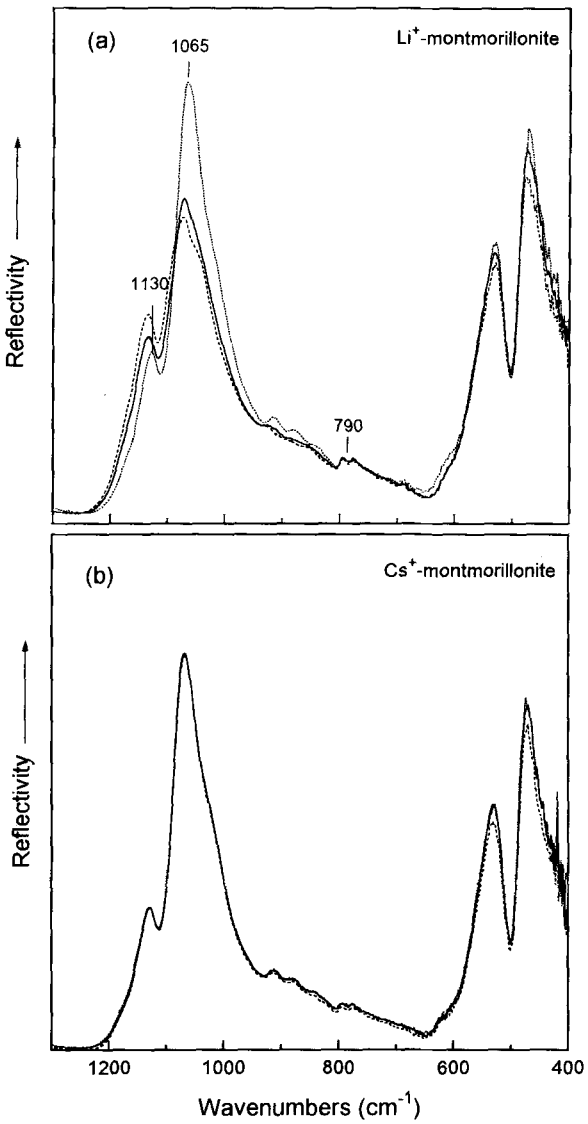


Figure 3. IR reflectance spectra of Li- (a) and Cs- (b) montmorillonites thermally treated at: 80 °C (·····), 180 °C (———) and 250 °C (– – –).

gested by one reviewer the band at 790 $cm^{-1}$ may arise from the presence of quartz inpurities.)

The reflectivity spectra of the Li- and Cs-montmorillonites after their heat treatment at various temperatures for 24 h were examined. Large variations in the reflectivity spectra with heat treatment were observed only for the Li-clay, as shown in Figure 3a. To demonstrate clearly the differences caused by this treatment, the spectra of the Li- and Cs-montmorillonites have been scaled to give the same intensity for the 790 $cm^{-1}$ band envelope. This band seems to be unaffected by heating and also by the KK analysis in terms of LO and TO modes, as illustrated in Figures 1c and 1d. The following changes in the Li-montmorillonite spectrum were observed: 1) The reflectivity maximum at 1065 $cm^{-1}$ was reduced upon heating, whereas the peak at 1130 $cm^{-1}$ moved to higher frequency (1135 $cm^{-1}$) and also increased in intensity. 2) The OH bending bands in the region 800–950 $cm^{-1}$ decreased in intensity and shifted to higher frequencies. From the spectra, it is obvious that thermal treatment affects the relative intensities and peak positions of the Si-O bands more than those of the hydroxyl librational vibrations. For this reason, emphasis is placed on the high-frequency vibrations of the spectra. In contrast with the Li-montmorillonite spectrum, the Cs-montmorillonite spectra remained unaffected by heating, as shown clearly in Figure 3b. The Kramers–Krönig analysis of heat-treated Li-montmorillonite provided the calculated LO and TO spectra (Figure 4). The spectra that are presented as $Im(-1/\epsilon^*)$ vs. frequency present significant differences in the frequency range 1000–1300 $cm^{-1}$. The LO spectrum of the sample dried at 80 °C exhibits 2 peaks at approximately 1148 and 1100 $cm^{-1}$ and a shoulder near 1175 $cm^{-1}$. Upon heating, this shoulder gains intensity, Figure 4b, and finally becomes the dominant band of the spectrum. The part of the spectrum between 400 and 1000 $cm^{-1}$ does not change with thermal treatment. The TO spectrum (Figure 4a) shows similar behavior; a shoulder at the high-frequency side of the 1050 $cm^{-1}$ band develops upon heating above 100 °C and becomes the strongest band (1065 $cm^{-1}$) after heating at 250 °C for 24 h.

The presence of the TO/LO pair of bands in this spectral region has also been observed in the $\epsilon''$ and $Im(-1/\epsilon^*)$ spectra of the amorphous silica and gel-derived $SiO_2$. Previous studies by Gaskell and Johnson (1976), Lucovsky et al. (1983), Pai (1986) and Kirk (1988) have attributed these bands to the asymmetric stretch (AS) of the Si-O-Si bridges in which the motion of the oxygen atom parallel to the Si-Si direction gives rise to 2 vibrational modes: 1) an $AS_1$ mode in which adjacent oxygen atoms execute the asymmetric stretch in phase with each other, and 2) an $AS_2$ mode in which adjacent oxygen atoms execute the asymmetric motion 180° out of phase. The $AS_2$ mode is optically inactive and can be activated only by coupling with the strong $AS_1$ mode (Kirk 1988). Almeida et al. (1990) and recently Kamitsos et al. (1993) have suggested that the coupling of these modes is stronger in $SiO_2$ gels compared to vitreous silica, probably because the Si-O-Si bridges are strained at the surface of the gel pores. In the frame of the above considerations, it is attributed to the observed bands in LO and TO spectra of clays to the 2 different types of oxygen motion during the asymmetric stretching of the Si-O-Si bridges. The strong peaks at 1050 and 1148 $cm^{-1}$ are ascribed to the in-phase motion of the oxygen ($AS_1$ mode) while the weak peaks at 1100 and 1125 $cm^{-1}$

https://doi.org/10.1346/CCMN.1997.0450504 Published online by Cambridge University Press

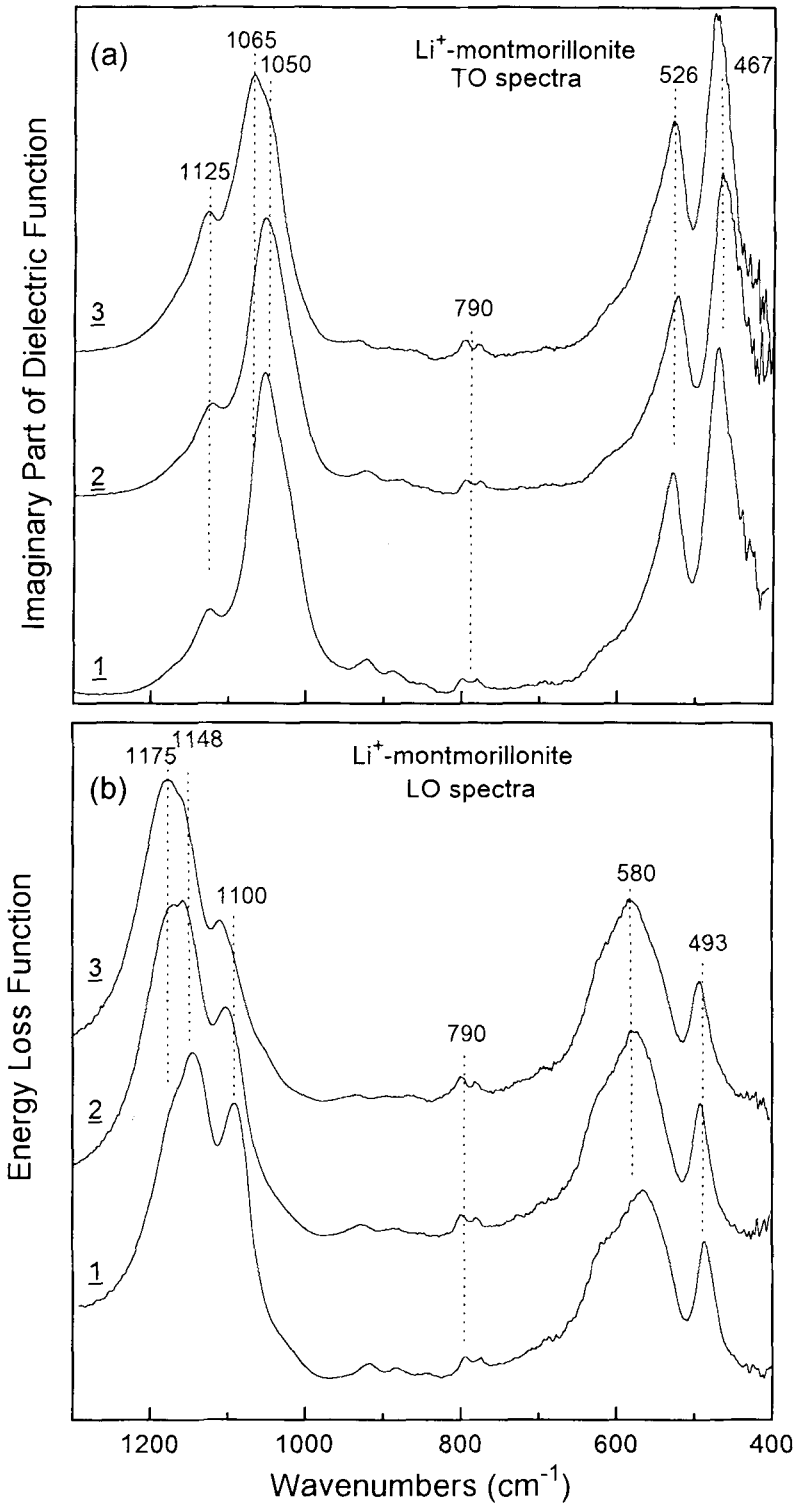


Figure 4. IR dielectric constant, $\epsilon''$ (a) and energy loss function, $\mathrm{Im}(-1/\epsilon)$ (b) of Li-montmorillonite thermally treated at 80 °C (1), 180 °C (2) and 250 °C (3).

https://doi.org/10.1346/CCMN.1997.0450504 Published online by Cambridge University Press

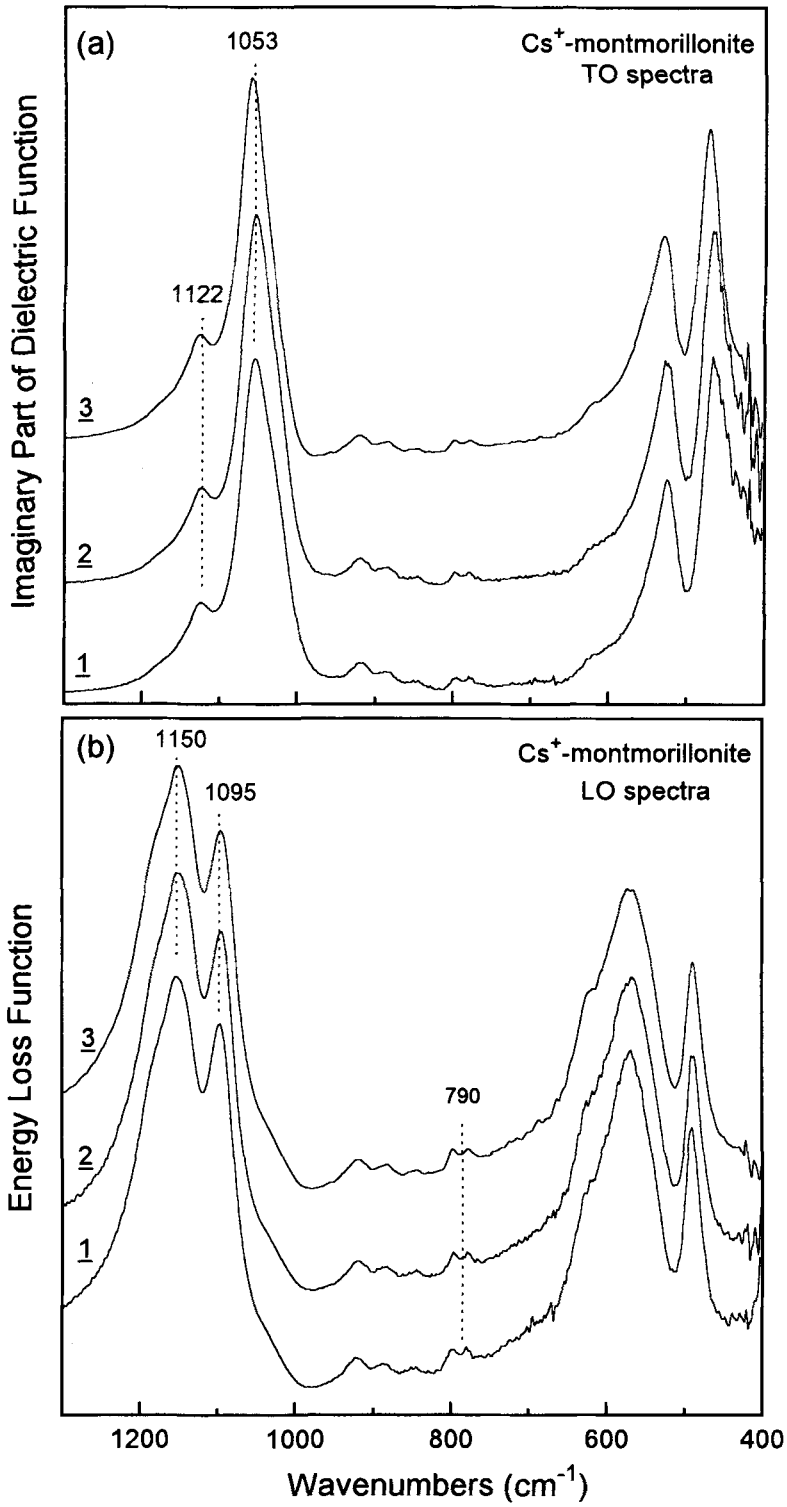


Figure 5. IR dielectric constant, $\epsilon''$ (a) and energy loss function, $\mathrm{Im}(-1/\epsilon)$ (b) of Cs-montmorillonite thermally treated at 80 °C (1), 180 °C (2) and 250 °C (3).

https://doi.org/10.1346/CCMN.1997.0450504 Published online by Cambridge University Press

($AS_2$ mode) to the 180° out-of-phase motion of oxygens.

A key question to be addressed with regard to the above reflectivity data is the origin of the 1175 and 1065 $cm^{-1}$ bands, the intensity of which changes drastically upon heating. It is well known that absorptions due to the Si-O vibrations in the spectra of clay minerals show more than 1 peak maxima. The splitting of the peaks is expected on account of the effect of the neighboring octahedral ions. Farmer and Russel (1964) have reported that, in dioctahedral minerals such as montmorillonite and beidellite, the IR active Si-O vibrations divide into 2 classes: those labelled $a_1$, which develop dipole moments perpendicular to the layer sheet (Si-$O_{apical}$), and those labelled $b_1$ and $b_2$, which have moments parallel to the layer sheet (Si-$O_{basal}$). The Si-$O_{apical}$ vibrations are observed at higher frequencies than the corresponding Si-$O_{basal}$ vibrations. Accordingly, we may ascribe the observed shoulders at 1175 and 1065 $cm^{-1}$ in the spectra of Li- and Cs-clays, Figures 4 and 5, to the Si-O-M vibrations (M = Fe, Al, Mg and O = apical). It should be also noted that heating affects only the TO or LO spectra of $Li^+$ and not of Cs-montmorillonite, Figures 5a and 5b. Because the only structural difference between the clay samples lies in the specific interlayer cation ($Li^+$ or $Cs^+$), it is concluded that the above effects are directly related to the ability of the interlayer cations to migrate into the octahedral frame during heating. In fact, large cations such as Cs (ionic radius 1.65 Å) cannot enter into the hexagonal holes (with diameter ~ 2.6 Å) to fill the available octahedral vacancies (McBride et al. 1975). Thus, it is not suprising that the IR spectrum of Cs-clay remains unaffected by the heat treatment. On the other hand, the smaller Li (ionic radius 0.78 Å) can enter into the hexagonal holes, after the water of hydration is removed by heating, and can probably be hosted in empty octahedral sites (size of the octahedral space ~1.32 Å). In this way the Li cations can approach and interact with the negative charge of the octahedral layer. These interactions can have pronounced effects on the Si-O vibrations. Recently Kitajima et al. (1990, 1991) studied the effects of layer charge on the IR spectra of synthetic fluorine micas. They found that the frequency of the Si-O vibrations was influenced by the field strength of the intelayer cation or by the specific ion in the lattice. The authors argue that changes in the restoring forces between silicon and oxygens, generated by variations in the layer charge, cause in turn frequency shifts in the IR spectra. We propose here a similar explanation based on the degree of the layer charge. The migration of the $Li^+$ cations into the layer structure strengthens its interaction with the negative charge of the octahedral layer and brings a decrease in the restoring forces between the $Mg^{2+}$ or $Fe^{2+}$ ions and the surrounding oxygens. Any changes in the restoring forces will be reflected in the frequency of the Si-$O_{apical}$ bands. Moreover, we note that the intensity of the Si-O-M vibrations is enhanced as the temperature of the treatment increases, Figure 4. This dependence can be explained by the increased number of $Li^+$ ions migrating into the layer structure. This is in agreement with the findings of Calvet and Prost (1971) who observed that the number of small cations migrating into a clay structure increases with increasing the temperature or the time of heat treatment. Furthermore, Madejová et al. (1996) have observed that heating of Li-montmorillonite above 150 °C brings changes in the IR spectrum such as the appearance of new bands at 1120 and 419 $cm^{-1}$, characteristic of pyrophyllite mineral that were attributed to Li fixation into octahedral sites. Alternatively, the $Li^+$ cations that remain in the interlayer space after the interlayer water is removed by heating can move closer to the basal oxygens of the tetrahedral layer and interact more strongly with them. However, such interactions should have a small effect on the Si-$O_{basal}$ vibrations, because the number of the interlayer $Li^+$ cations remaining in the intercrystalline zone after thermal treatment is small, as illustrated by the small shift of 1100 $cm^{-1}$ band to higher frequencies, Figure 4.

## CONCLUSIONS

The reflectivity spectra of Li- and Cs-montmorillonite heat-treated at various temperatures were measured at oblique incidence (10° off-normal). Kramers–Krönig analysis of these spectra allowed the detection of the TO and LO modes of vibration of Si-O-Si bridges. As a result of this analysis, a pair of bands in the high-frequency part of the TO ($\epsilon''$) and LO ($-\mathrm{Im}(1/\epsilon^*)$) spectra were found which can be understood in terms of a 2-vibrational-modes model proposed previously for amorphous silica. Heat treatment of Li-clay samples caused large variations in the corresponding IR reflectance spectra. The major change in the TO and LO spectra with increasing treatment temperature was the systematic development of a new pair of bands. These bands were attributed to the AS vibrational mode of Si-O-M bridges (M = $Fe^{2+}$, $Mg^{2+}$, $Al^{3+}$ after neutralization of the lattice charge by migrated $Li^+$ cations. The results lead to a better understanding of the Hofmann–Klemen effect because the silicon-oxygen vibrations were strongly affected by the ability of small interlayer cations to migrate to the clay framework.

## ACKNOWLEDGMENTS

The authors would like to express their appreciation to J. Koutselas for supplying us with a copy of the computer program for KK analysis.

## REFERENCES

Almeida RM, Guiton TA, Pantano CG. 1990. Characterization of silica gels by infrared reflection spectroscopy. J Non-Cryst Solids 121:193–197.

Alvero R, Alba MD, Castro MA, Trillo JM. 1994. Reversible migration of lithium in montmorillonite. J Phys Chem 98: 7848–7853.

Berreman DW. 1963. Infrared absorption at longitudinal optic frequency in cubic crystal films. Phys Rev 130:2193–2198.

Bishop JL, Pieters CM, Edwards JD. 1994. Infrared spectroscopic analyses on nature of water in montmorilonite. Clays Clay Miner 42:702–716.

Calvet R, Prost R. 1971. Cation migration into empty octahedral sites and surface properties of clays. Clays Clay Miner 19:175–186.

Clark RN, King TV, Kleijwa M, Swayze GA. 1990. High spectral resolution reflectance spectroscopy of minerals. J Geophys Res 95:12653–12680.

Delineau T, Allard T, Muller JP, Barres O, Yvon J, Cases JM. 1994. FTIR reflectance vs. EPR studies of structural iron in kaolinites. Clays Clay Miner 42:308–320.

Farmer VC. 1974. The layer silicates. In: Farmer VC, editor. The infrared spectra of minerals. London: Mineral Soc. p 331–363.

Farmer VC, Russel JD. 1964. The infrared of layered silicates. Spectrochim Acta 20:1149–1173.

Farmer VC, Russel JD. 1967. Infrared absorption spectrometry in clay studies. Clays Clay Miner 15:121–142.

Galeener FL, Lucovsky G. 1976. Longitudinal optical vibrations in glasses: $GeO_2$ and $SiO_2$. Phys Rev Lett. 37:1474–1478.

Gaskell PH, Johnson DW. 1976. The optical constants of quartz, virteous silica and neutron-irradiated virteous silica: II. J Non-Cryst Solids 20:171–191.

Hofmann V, Klemen R. 1950. Verlust der Austausch fohiqkeit von Lithiumionen and Bentonit durch Erhitzung. Z Anorg Allg Chem 262:95–99.

Kamitsos EI, Patsis AP, Karakassides MA, Chryssikos GD. 1990. Infrared reflectance spectra of lithium borate glasses. J Non-Cryst Solids 126:52–67.

Kamitsos EI, Patsis AP, Kordas G. 1993. Infrared-reflectance spectra of heat-treated, sol-gel derived silica. Phys Rev B 48:12499–12505.

King RD, Noceda DG, Pinnavaia TJ. 1987. On the nature of electroactive sites in clay-modified electrodes. J Electroanal Chem 236:43–53.

Kirk CT. 1988. Quantitative analysis of the effect of disorder-induced mode coupling on infrared absorption in silica. Phys Rev B 38:1255–1273.

Kitajima K, Takusagawa N. 1990. Effects of tetrahedral isomorphic substitution on the IR spectra of synthetic fluorine micas. Clay Miner 25:235–241.

Kitajima K, Taruta S, Takusagawa N. 1991. Effect of layer charge on the IR spectra of synthetic fluorine micas. Clay Miner 26:435–440.

Lerot L, Low PF. 1976. Effect of swelling on the infrared absorption spectrum of montmorillonite. Clays Clay Miner 24:191–199.

Lucovsky G, Wong CK, Pollard WB. 1983. Vibrational properties of glasses: Intermediate range order. J Non-Cryst Solids 59+60:839–846.

Madejová J, Bujdák J, Gates WP, Komadel P. 1996. Preparation and infrared spectroscopic characterization of reduced-charge montmorillonite with various Li contents. Clay Miner 31:233–241.

McBride MB, Pinnavaia TJ, Mortland MM. 1975. Structural $Fe^{3+}$ in smectites by exchange ions. Clays Clay Miner 23: 103–107.

Minami T. 1983. Preparation and properties of superionic conducting glasses based on silver halides. J Non-Cryst Solids 56:15–26.

Pai PG, Chao SS, Takagi Y, Lucovsky G. 1986. Infrared spectroscopic study of silicon oxide ($SiO_x$) films produced by plasma enhanced chemical vapor deposition. J Vac Sci Technol A 4:689–694.

Roy BN. 1987. Spectroscopic analysis of the structure of silicate glasses along the joint $xMAlO_2$-$(1-x)SiO_2$ (M = Li, Na, K, Rb, Cs). J Am Ceram Soc 70:183–192.

Russel JD, Fraser AR. 1971. I.R. Spectroscopic evidence for interaction between hydronium ions and lattice OH groups in montmorilonite. Clays Clay Miner 19:55–59.

Spitzer WG, Kleinman DA. 1961. Infrared lattice bands of quartz. Phys Rev 121:1324–1335.

Spitzer WG, Miller RC, Kleinman DA, Howarth LE. 1962. Far infrared dielectric dispersion in $BaTiO_3$, $SrTiO_3$ and $TiO_3$. Phys Rev 126:1710–1721.

Sposito G, Prost R, Gaultier JP. 1983. Infrared spectroscopic study of absorbed water in reduced charged Na/Li-montmorillonites. Clays Clay Miner 31:9–16.

Stern F. 1963. Elementary theory of the optical properties of solids. Solid State Phys 15:299–408.

Wihlborg WT. 1989. Applications of reflectance FT-IR microspectroscopy. Scan Time 16:1–5.

*Received 24 July 1996; accepted 12 October 1996; Ms. 2793)*